

**GROUND-BASED SIMULATION OF LOW EARTH ORBIT PLASMA CONDITIONS:
PLASMA GENERATION AND CHARACTERIZATION**

Session 2: Ground Testing Techniques

John D. Williams,* Casey C. Farnell,‡ and Paul B. Shoemaker†
Colorado State University
Fort Collins, CO 80523
johnw@engr.colostate.edu

Jason A. Vaughn§ and Todd A. Schneider§
NASA Marshall Space Flight Center
Huntsville, AL 35812

Abstract

A 16-cm diameter plasma source operated on argon is described that is capable of producing a plasma environment that closely simulates the low Earth orbit (LEO) conditions experienced by satellites in the altitude range between 300 to 500 km. The plasma source uses a transverse-field magnetic filter, and has been successful in producing low electron temperature plasmas that contain streaming ion populations. Both of these characteristics are important because the plasma in LEO is relatively cold (e.g., $T_e \sim 0.1$ eV) and the ram energy of the ions due to the motion of the satellite relative to the LEO plasma is high (e.g., 7,800 m/s which corresponds to ~ 5 eV for O^+ ions). Plasma source operational conditions of flow rate and discharge power are presented that allow the electron temperature to be adjusted over a range from 0.14 to 0.4 eV. The expanding plasma flow field downstream of the source contains both low-energy, charge-exchange ions and streaming ions with energies that are adjustable over a range from 4 eV to 6 eV. At low flow rates and low facility pressures, the streaming ion component of the ion population comprises over 90% of the total plasma density. In the work described herein, a large area retarding potential analyzer was used to measure both electron and ion energy distribution functions in the low density, expanding plasma produced downstream of the plasma source. The benefits of using this type of plasma diagnostic tool in easily perturbed, low-density plasma are identified, and techniques are also discussed that can be used to perform real-time measurements of electron temperature. Finally, recommendations are made that may enable lower electron temperatures to be produced while simultaneously decreasing the plasma source flow rate below 1 to 2 sccm.

* Assistant Professor, Mechanical Engineering Dept.

‡ Graduate Research Assistant, Mechanical Engineering Dept.

† Undergraduate Laboratory Assistant, Mechanical Engineering Dept.

§ Research Scientist, Environmental Effects Laboratory

Introduction

Simulation of the LEO plasma environment in ground-based vacuum facilities has been performed at various governmental space agencies and commercial aerospace companies for many years.^{1,2,3,4} In most of these studies compromises have been made on the fidelity of the plasma environment simulations in regard to plasma composition, plasma density, electron temperature, and ram (or streaming) ion energy. M.G. Cho et al.⁵ used an argon ion source to simulate the LEO plasma environment ($n_e = 0.5 \times 10^6 \text{ cm}^{-3}$) during high voltage solar cell arc tests where the reported electron temperature produced by their LEO plasma simulator was quite high at 2.4 eV compared to actual LEO electron temperatures of ~ 0.1 eV. Vaughn et al.⁶ present results of studies on arcing in plasma and expansion of arcs into simulated LEO ambient plasmas produced by an orificed hollow cathode discharge operated on argon. The plasma density in this study was $1.5 \times 10^6 \text{ cm}^{-3}$ and the electron temperature was 1 eV at the sample location. In earlier work, Konradi et al.⁷ discuss plasma ion current collection on panels of various sizes biased at large negative voltages. The plasma was created in a large vacuum test facility using a Kaufman ion source which was also operated on argon. No biases were applied to the ion optics system, and, consequently, the energy distribution of the emitted ions was only dependent upon the plasma potential distribution within the discharge chamber and the potential variation from the source to the panels under test. The authors indicate that electron temperatures as low as 0.15 eV were obtained at plasma densities ranging from $0.5 \times 10^6 \text{ cm}^{-3}$ to $2.5 \times 10^6 \text{ cm}^{-3}$, but that the ion flow field was dominated by low energy charge exchange ions that did not simulate orbital ram energies very well. Kern and Bilén⁸ performed plasma current collection studies on breaches in wire insulation using a low energy plasma source where the plasma density and temperature at their sample location was $\sim 1 \times 10^7 \text{ cm}^{-3}$ and 1 eV, respectively. In their work, they report that the argon ions were streaming from the plasma source at energies of ~ 20 eV. Choiniere et al.⁹ report on plasma electron collection to surfaces exposed to a high velocity xenon ion flow fields of 25 to 50 eV. The electron temperature in their experiments was measured to be 1.4 to 1.8 eV at quite high electron densities that were varied over a range from $0.5 \times 10^9 \text{ cm}^{-3}$ to $4 \times 10^9 \text{ cm}^{-3}$.

The low electron temperature plasma source we describe in this paper utilizes a transverse-field magnetic filter. It is well known that plasma sources equipped with magnetic filters are capable of producing plasmas with unique properties. Magnetic filters have been exploited in neutral hydrogen injectors for fusion research^{10,11} and in atomic nitrogen and oxygen ion sources for plasma processing applications.^{12,13} Magnetic filter-equipped plasma sources that use multi-cusp magnetic field configurations are also finding applications as ion sources in focused ion beam (FIB) lithography systems because they are capable of producing very low-energy-spread ion beams with correspondingly high emittance.¹⁴ These FIB plasma sources exhibit very low electron temperatures on the order of 0.1 eV in the region downstream of the magnetic filter and careful design of the filter layout and discharge chamber magnetic fields enables ion beams to be produced from plasma with ion energy spreads that are as low as 0.6 eV.¹⁴

To a very large extent, the plasma simulation facilities described in Refs. (1) through (9) have performed their task well, and results from these and other activities have guided the design and fabrication of both materials and hardware used in space flight applications. However, two problems have persistently plagued LEO simulation efforts and they include (1) difficulty in

obtaining plasma sources that produce plasmas with adjustable, ultra-low electron temperatures on the order of 0.1 eV and streaming ion populations of 5 eV and (2) poor performance of plasma diagnostic equipment due to contamination buildup on probe surfaces, very large sheath growth at negative biases, or probe-induced perturbations at positive biases. Recent results obtained from the International Space Station (ISS) have indicated that electron current collection on positively biased solar cells may increase under low electron temperature conditions.¹⁵ It would be desirable to study this phenomenon in the laboratory under well controlled conditions, and our paper describes proof-of-concept experiments that have been performed on a LEO plasma simulator based on magnetic filters that could enable this sort of testing. We also describe the use of a large-area, multi-gridded retarding potential analyzer (RPA) manufactured by EPL, Inc. that was used to characterize the electron and ion energy distribution functions in the low-density, expanding-plasma environment downstream of the plasma source. The benefits of using RPAs to measure expanding, low-density plasma properties are also discussed, and rf techniques are reviewed that would be useful for performing rapid measurements of electron temperature.

Apparatus and Procedures

Figures 1a and 1b contain photographs and schematic diagrams of our experimental setup. All testing was performed in a 1.2 m diameter by 5 m long stainless steel vacuum chamber that was pumped with a 0.9-m diameter, 20-kW diffusion pump. The base pressure of this facility with no flow was 1×10^{-6} Torr after 1 to 2 hr pump down times, and argon flow rates of 15 sccm increased the vacuum pressure to about 2×10^{-5} Torr. The magnetic filter-equipped plasma source is shown in the upper left and right hand photographs in Fig. 1a and on the left hand side of the schematic diagram shown in Fig. 1b. The photograph of the operating plasma source was taken through the view port shown in the lower left photograph, which only allowed for a partial image of the annular plasma emission region. The discharge chamber of the plasma source was 22 cm in diameter, and the active area of the ion optics system placed on the downstream end of the source was 16 cm. Although capable of extracting an ion beam, the multi-aperture, three-grid ion optics system was only used to reduce the open area of the source and increase the neutral density within the discharge chamber. An electrical and mechanical schematic diagram of the plasma source is displayed in Fig. 2a where the magnetic filter structure is shown immediately upstream of the ion optics system. A plasma is created within the discharge chamber by introducing argon flow to the source and by using a power supply connected between a hot filament cathode and an anode structure. Typical anode voltages of 35 to 55 V were investigated over discharge current ranges from 0.6 to 3 A. As indicated in Fig. 2a, the anode of the plasma source was connected to vacuum chamber ground for all testing described in this paper. In addition, the body of the plasma source including the magnetic filter was electrically connected to ground.

The discharge plasma contains both high-energy primary electrons and a Maxwellian electron group ($T_e \sim 2$ to 7 eV). Ions from the discharge plasma drift toward the magnetic filter structure and pass through into the region downstream of the filter, and they drag along low energy electrons with them. The magnetic field strength in the central regions of the magnetic filter region was ~ 45 Gauss for most of the testing described herein. Energetic electrons within the discharge chamber are prevented from following the ions due to the filtering effect of the radial magnetic field generated between the inner and outer magnet rings of the filter.¹⁶ Although the magnetic field is strong enough to stop energetic discharge electrons, it is not

strong enough to stop plasma from leaking through this region. The low energy electrons are able to diffuse through the filter (and follow the ions) via momentum exchange collisions amongst other low energy electrons, neutrals, ions, and possibly through other mechanisms. A large area retarding potential analyzer (RPA) manufactured by EPL, Inc was placed 61 cm downstream of the plasma source as shown in Figs. 1a and 1b. The RPA was used to characterize the plasma flow field properties. An electrical schematic of the RPA is shown in Fig. 2b. The RPA uses three aligned grids that are spaced relatively far apart from one another for improved energy resolution purposes. However, the apertures in the grids are comprised of slots with widths that are only slightly smaller than the grid-to-grid separation distance. An analysis of the RPA design using SIMION 7.0 suggested that the potential within the apertures of the grid used to discriminate ion energy was varying significantly from the potential applied to the grid under some bias conditions. It was felt that the potential variation across the apertures could cause inaccurate energy distribution functions to be measured, and, in order to correct this problem, a high transparency (90%) nickel mesh manufactured by Buckbee-Mears was placed over the apertures of the grid located adjacent to the collector electrode. This change resulted in significantly improved performance of the RPA where ion and electron energy distribution characteristics less than 0.1 eV could be easily resolved.

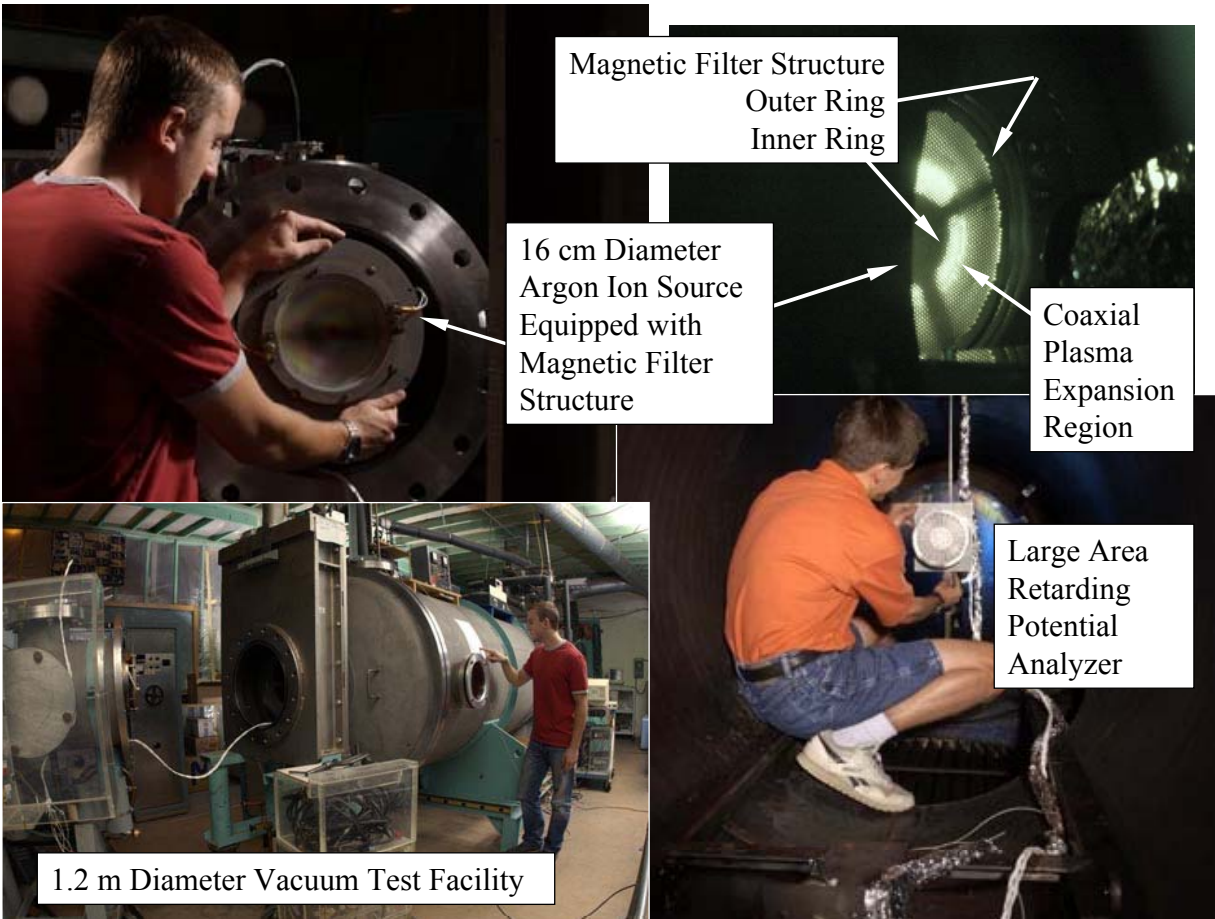


Fig. 1a Photographs of test setup.

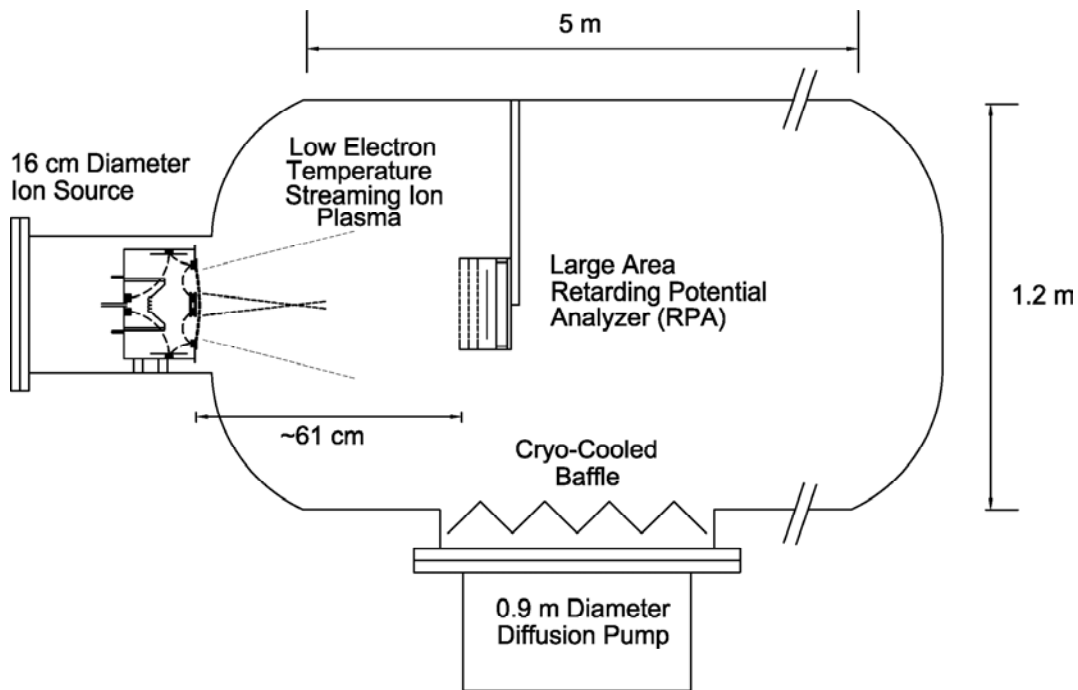


Fig. 1b Schematic diagram of LEO plasma simulation test facility.

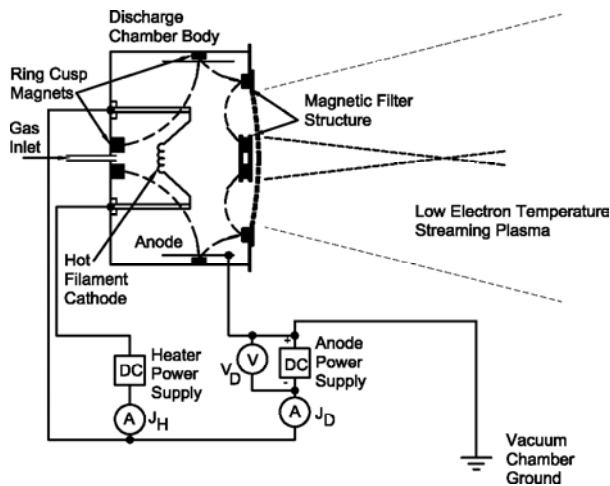


Fig. 2a Schematic of magnetic filter-equipped plasma source.

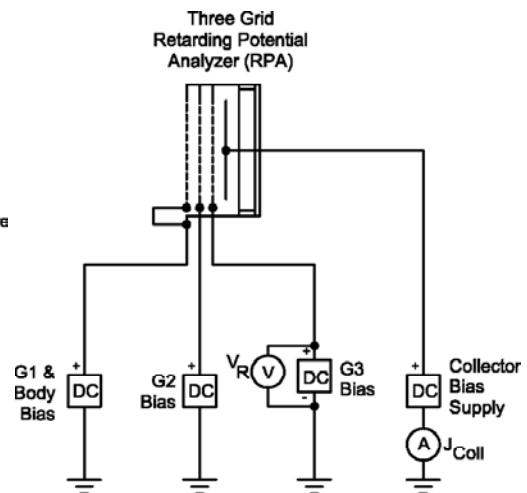


Fig. 2b Schematic of RPA

As configured for our tests, the RPA depicted in Figs. 1 and 2 is capable of providing high-resolution measurements of both ion and electron energy characteristics. RPAs are relatively inexpensive to build and easy to operate, and data analysis is simple compared to the analysis of Langmuir probe data due to the removal of the ion current from the sampling electrode when operated in the electron energy characterization mode. RPAs can also be used in non-uniform plasmas (i.e., freely expanding ones where plasma density varies with position) or

in vacuum facilities that are not ultra clean without the concern that accompanies Langmuir probes.¹⁷ This is a consequence of the energy selection grid being located within the device where it will not cause varying ion or electron sheaths to form and grow as it is being biased. RPAs are also more tolerant of contamination than Langmuir probes because charged particle collection occurs within RPAs on electrodes that are biased at relatively high potentials.

In addition to a low electron temperature, the plasma region downstream of the magnetic filter also contains a streaming ion population that is relatively mono-energetic at an energy that can range from ~ 4 eV to 6 eV depending upon plasma source operational conditions like flow rate, discharge power, discharge voltage, and discharge plasma uniformity. Although not confirmed at this time, it is believed that the streaming ions gain their energy through plasma expansion processes as the plasma density decreases from a relatively high value just downstream of the plasma source to much lower densities at distances further downstream. Some charge exchange ions are also created as ions stream from the source, but their relative numbers are low (less than 10%) and can be further minimized by reducing the flow rate required by the plasma source, and, thereby dropping the facility neutral background pressure.

As mentioned above, Fig. 2b contains an electrical schematic of the three-grid RPA that was used to measure both ion and electron energy characteristics. For electron energy characterization, the grid adjacent to the plasma was typically held at a constant potential that was slightly above plasma potential (~ 1 V). The next grid further into the RPA was typically held at +19 V to accelerate electrons from the plasma that pass through the first grid and to repel plasma ions from penetrating into regions located further into the RPA. The third grid from the plasma is used to energy select the electrons that pass through the second grid. At a given potential, this grid will allow electrons with an energy greater than this potential to pass through, but it will stop or retard all other electrons with insufficient energy to surmount this “retarding” potential. The collector electrode is typically biased positive of the discriminating grid (i.e., grid # 3) to avoid secondary electrons produced at the collector electrode from leaving this surface and flowing toward the third grid or other surfaces located within the RPA. A typical RPA data set consists of a list of the potentials applied to the first grid, second grid, and the collector electrode along with measurements of the collector current versus the potential applied to the third grid. A log-linear plot of the collector current versus the retarding potential can be used to estimate properties like plasma density, plasma potential, and electron temperature and/or energy. As mentioned above, one unique feature of RPA data collected with the set up shown in Fig. 2 is the automatic removal of the ion current. This simplifies the analysis of the current-voltage trace and also enables other more subtle plasma diagnostic techniques to be performed.

One novel use of an RPA can be implemented by superimposing an alternating sinusoidal voltage signal onto the retarding electrode as shown in Fig. 2 and described by Gill and Webb.¹⁸ If implemented properly, this alternating voltage signal would cause the collector current to be modulated in a way that could be used to determine the electron temperature or electron energy distribution function.¹⁹ It is noted that AC modulation techniques applied to Langmuir probes and RPAs have been performed since the 1930s. However, AC modulation of RPA energy discrimination electrodes has never been mentioned to our knowledge in the context of characterizing low-density plasmas that may be appropriate for producing LEO-like plasma environments. In addition, plasma properties of non-uniform, expanding plasmas may be characterized by applying AC modulation techniques to RPAs that would be impossible to implement using Langmuir probes because of non-linear ion current collection effects caused by excessive sheath growth at negative biases in flowing, low density plasmas.

Application of an AC signal to the retarding grid of an RPA will partially rectify the collector current signal due to the exponential dependence of electron current on retarding potential. Analysis of the collector current frequency spectrum is then used to find the magnitudes of the first and second harmonics that are induced by the voltage waveform imposed on the retarding grid and the rectification effects, respectively. Similar to AC modulation of Langmuir probes, the RPA modulation technique would use the ratio of 2nd-to-1st harmonic amplitudes to determine the electron temperature. We plan to explore the use of AC modulation techniques in future work on low electron temperature, expanding plasmas in order to develop a faster method of determining electron temperature compared to methods that involve current-voltage data acquisition and subsequent analysis.

As mentioned above, the RPA was also used to measure ion energy characteristics. For these measurements, the grid adjacent to the plasma was typically held at a constant potential that was below plasma potential by 2 to 5 V. The next grid further into the RPA is typically held at -28 V to accelerate ions from the plasma that pass through the first grid and to repel plasma electrons from penetrating into regions located further into the RPA. The third grid from the plasma is used to energy select the ions that pass through the second grid. At a given potential, this grid will allow ions with an energy greater than this potential to pass through, but it will stop or retard all other ions with insufficient energy to surmount this “retarding” potential. The collector electrode is biased negative of the discriminating grid (i.e., grid # 3) to collect ions that make it past the third electrode. The derivative of the RPA trace was used to determine the ion energy distribution function. It is noted that Auger (or secondary) electron emission from the stainless steel collector electrode can occur and these electrons will flow to the discriminator electrode when it is biased positive of the collector. For argon ions, this effect can account for up to 20% of the measured ion current signal.

Results

A typical RPA electron trace is shown in Fig. 3 on both linear and log scales for the y-axis. This trace was taken at a relatively high plasma source flow rate of 73 sccm when the discharge voltage was set to 45 V and the discharge current was set to 2.2 A. Although not evident on the linear trace, a slight dc leakage current was detected and subtracted from the trace before plotting the data on the log scale. The break in the slope of the log trace at ~ 0.1 V is used to infer plasma potential, which was consistent with RPA ion trace data as described below. Once the current offset was removed, the log trace was fit to a straight line whose slope yielded an electron temperature of 0.14 eV. These same data were collected over a range of flow rates from 6 to 74 sccm (Ar), and the corresponding electron temperatures are plotted versus flow rate in Fig. 4. The electron temperature was observed to increase from 0.14 eV at high flow conditions to a value just above 0.35 eV at 6 sccm.

A study was also conducted to determine the effects of discharge voltage and current on electron temperature. The results of these tests are shown in Fig. 5 when the flow rate to the plasma source was fixed at 14.7 sccm. A low discharge current of 0.6 A was observed to produce relatively high electron temperatures in the expanding plasma (~ 0.44 eV). As the discharge current was increased, however, the electron temperature decreased dramatically to a minimum value of 0.17 eV at a discharge voltage of 35 V and discharge current of 2.2 A. A relatively small effect of discharge voltage on electron temperature was observed in the preliminary experiments conducted to date, which was unexpected. Although more work needs

to be completed to understand the data presented in Figs. 4 and 5, we are encouraged by the ability to control the electron temperature by varying the plasma source operating conditions.

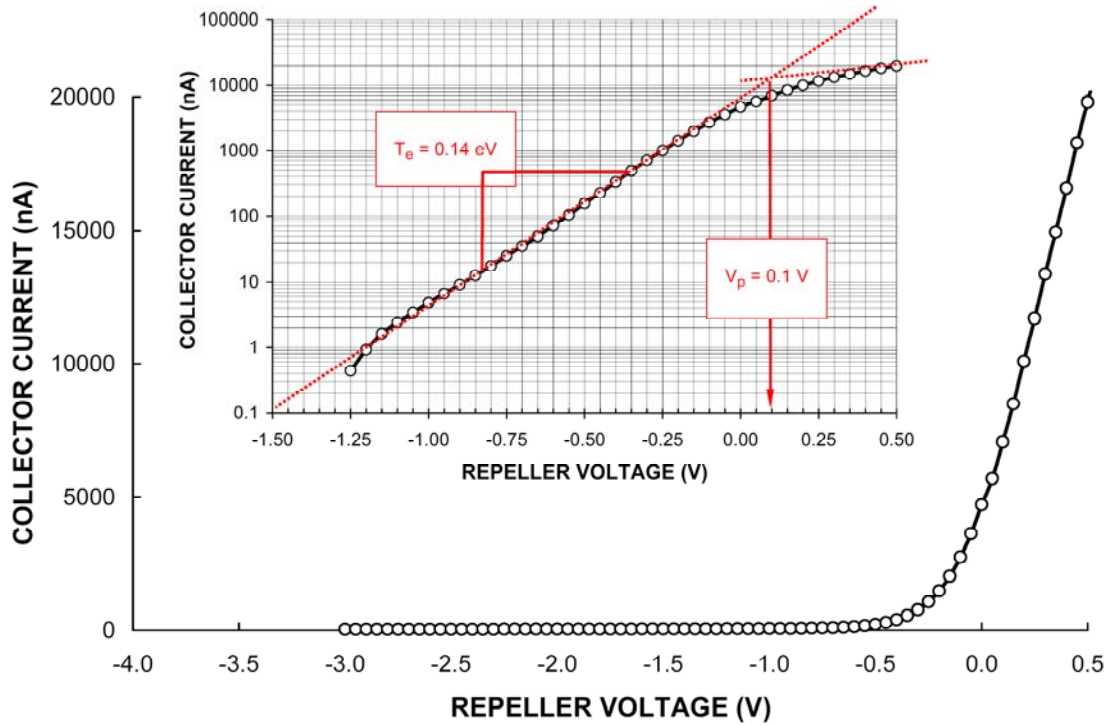


Fig. 3 Typical RPA electron trace plotted on linear and log scale.

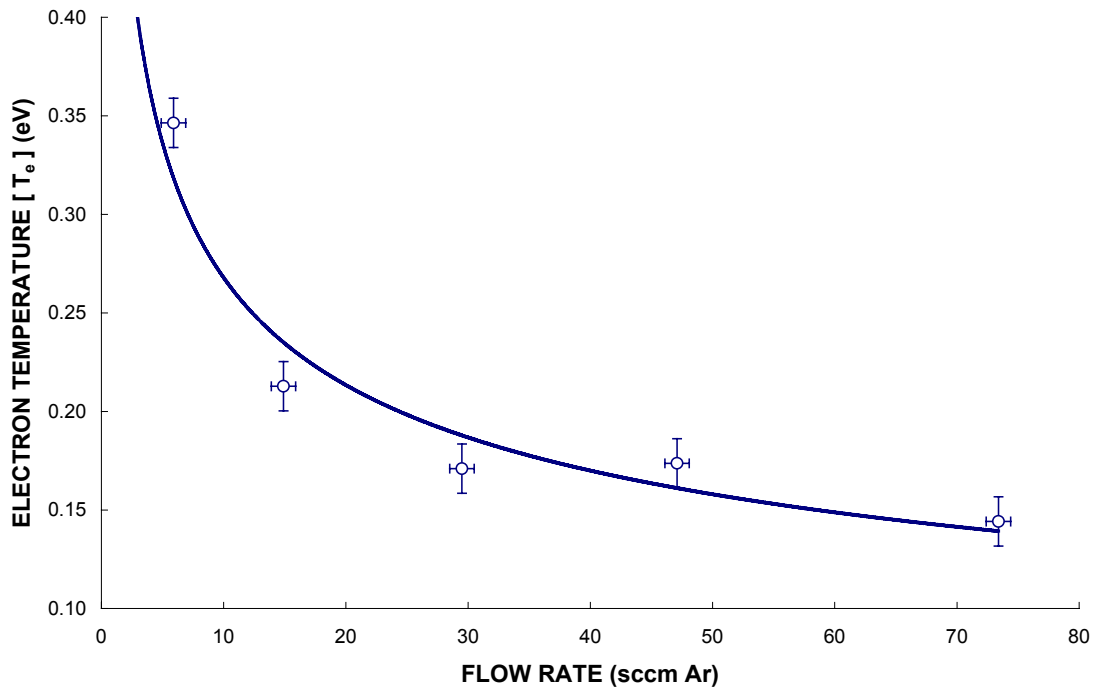


Fig. 4 Effect of flow rate on electron temperature at a fixed discharge power level of $\sim 90 \text{ W}$.

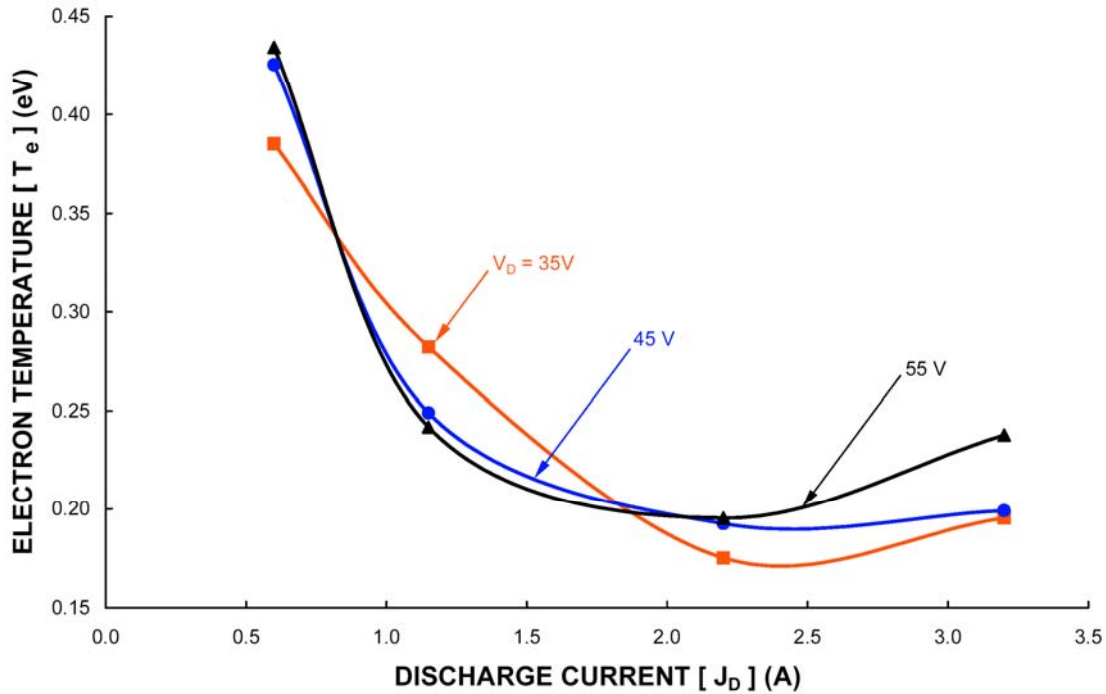


Fig. 5 Effects of discharge voltage and current on electron temperature in the expanding plasma.

Figure 6 contains an RPA ion trace taken in the expanding plasma region when the plasma source was operated at a flow rate of 14.9 sccm (Ar) and at a discharge voltage and current of 46 V and 2.2 A, respectively. The derivative of the trace is shown in the inset figure, which is representative of the ion energy distribution function. As shown in the figure, the ion flow field is comprised of two components. One component corresponds to low energy ions that are created at plasma potential from charge exchange reactions between neutrals and streaming ions. This ion component signal is identified in Fig. 6 at a potential of 0.3 V. As mentioned earlier, measurements of plasma potential using RPA electron traces agreed well with measurements based on the low energy charge exchange ion signal. The other ion component corresponds to ions produced in the plasma source at a higher potential that are accelerated into the lower density plasma regions downstream. The streaming ion density at the RPA was calculated to be $4 \times 10^5 \text{ cm}^{-3}$ by assuming that the RPA transparency to ions was 0.59 and the area of the RPA collector electrode was 65 cm^2 .

For the plasma source operating conditions of Fig. 6, the most probable streaming ion energy relative to the ambient plasma potential was 5 eV, and the full-width, half maximum (FWHM) energy spread of the streaming ions was 2 eV. Similar measurements of the most probable ion energy (relative to the ambient plasma potential) and FWHM energy spread were made at different discharge voltages and currents, and these data are shown in Fig. 7. The streaming ion energy is shown to vary from about 4 to 6 eV while the FWHM energy spread varies from about 2 to 3 eV as the discharge current is varied from 0.6 to 3 A. A slight trend of increased ion energy and energy spread was observed with increasing discharge voltage. The streaming ion energy of 5 eV and the plasma density of $\sim 4 \times 10^5 \text{ cm}^{-3}$ closely match the plasma conditions in LEO environments.

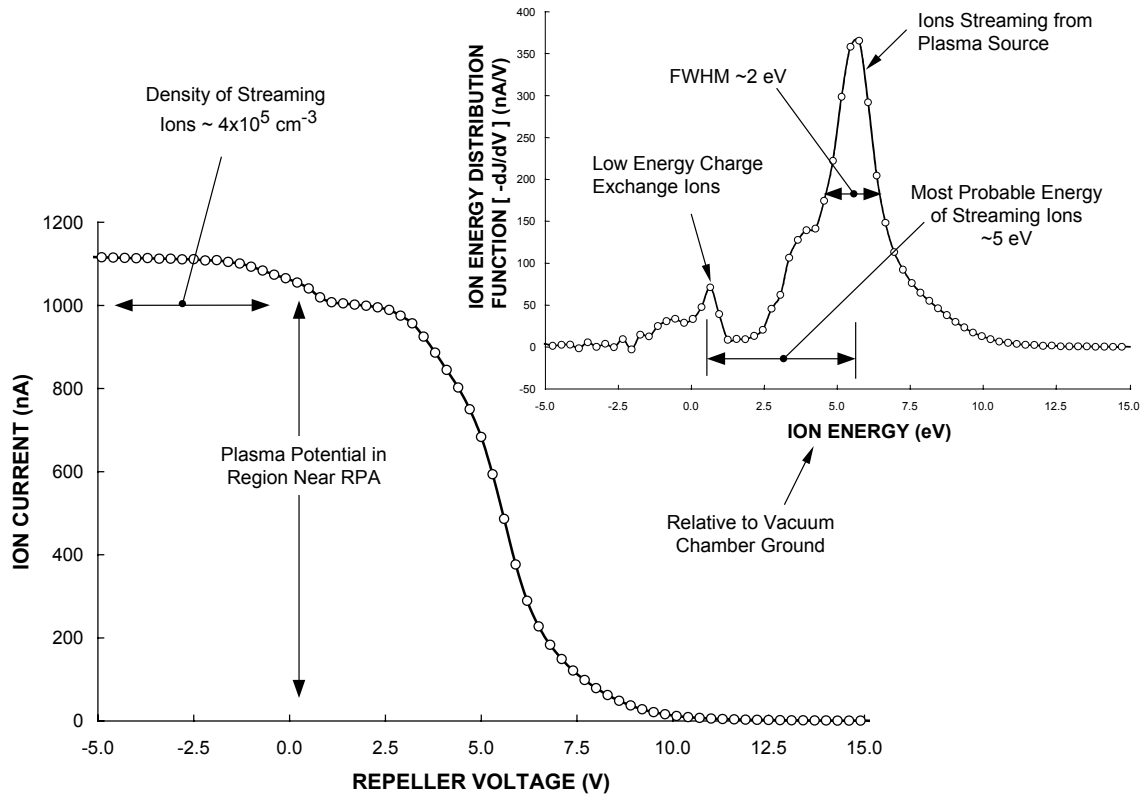


Fig. 6 Typical RPA ion current trace and corresponding ion energy distribution function that shows presence of charge exchange and streaming ion populations.

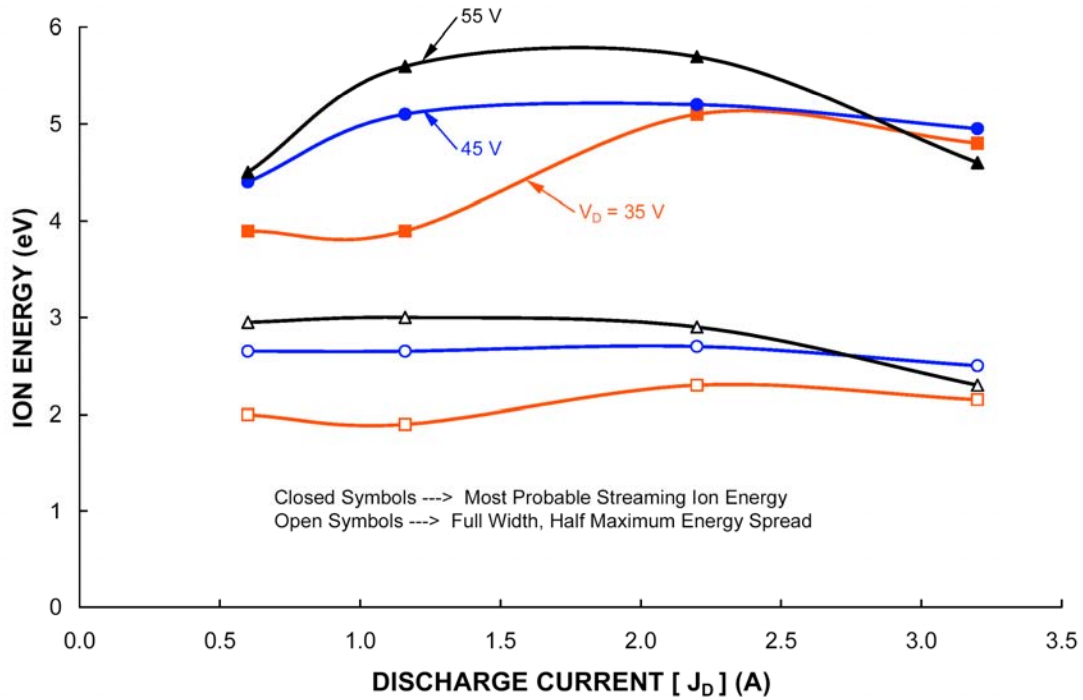


Fig. 7 Effect of discharge voltage and current on streaming ion energy and energy spread.

Conclusions and Recommendations for Future Work

The preliminary data presented herein suggests that a magnetic filter-produced expanding plasma represents an excellent candidate for use as a LEO plasma simulator in that it produces plasma with both low electron temperature and streaming ion energies. Operating conditions of flow rate, discharge current, and discharge voltage were shown to enable production of plasma electron temperatures over the range from 0.14 to 0.45 eV and streaming ion energies over the range from 4 to 6 eV. Increasing the flow rate to the plasma source was observed to have the greatest effect on reducing the electron temperature, which was probably due to increased neutral densities within the plasma source. One recommendation for future work would be to improve the gas seals in the source and to mask down the ion extraction region in an effort to increase the neutral density within the plasma source at a given flow rate condition. Increasing the neutral density near the magnetic filter structure by injecting the gas at this location might also have a beneficial effect of reducing the electron temperature below 0.14 eV. In this study, high quality electron and ion energy distribution functions were obtained from a unique, large-area retarding potential analyzer that could be operated without perturbing the low density plasma environment. One disadvantage of this type of plasma diagnostic is the time it takes to acquire and analyze the current-voltage trace. To address this concern, an ac-based technique was proposed to improve the speed in which electron temperature measurements are obtained, and further work to pursue this approach is also recommended.

Acknowledgements

The authors wish to thank Drs. Dale Ferguson and Boris Vayner of NASA Glenn Research Center for loaning their large area retarding potential analyzer instrument to CSU. Partial financial support for Mr. Casey Farnell and Mr. Paul Shoemaker was provided by Marshall Space Flight Center and is gratefully acknowledged. Special thanks go out to Mr. Justin Bult, Mr. Colin Olson, and Mr. Derek Reding for designing and fabricating the plasma source used in this study.

References

¹ H. Thiemann, and K. Bogus, "Anomalous Current Collection and Arcing of Solar-Cell Modules in a Simulated High-Density, Low-Earth-Orbit Plasma," *ESA Journal*, V. 10, 1986, pp. 43-57.

² J.T. Galofaro, et al., "Electrical Breakdown of Anodized Coatings in Low-Density Plasmas," *J. Spacecraft and Rockets*, V. 36, No. 4, 1999, pp. 579-585.

³ B.G. Herron, J.R. Bayless, and J.D. Worden, "High-Voltage Solar Array Technology," *J. Spacecraft*, V. 10, No. 7, 1973, pp. 457-462.

⁴ Banks, B.A., S.K. Rutledge, and J.A. Brady, "The NASA Atomic Oxygen Effects Test Program," 15th Space Simulation Conference, NASA CP-3015, Williamsburg, Virginia, Oct. 1988, pp. 51-65.

-
- ⁵ M.G. Cho, et al., "Plasma Response to Arcing in Ionospheric Plasma Environments: Laboratory Experiment," *J. Spacecraft and Rockets*, V. 39, No. 3, 2002, pp. 392-399.
- ⁶ J.A. Vaughn, et al., "Electrical Breakdown Currents on Large Spacecraft in Low Earth Orbit," *J. Spacecraft and Rockets*, V. 31, No. 1, 1994, pp. 54-59.
- ⁷ A. Konradi, B. McIntyre, and A.E. Potter, "Experimental Studies of Scaling Laws for Plasma Collection at High Voltages," *J. Spacecraft*, Vol. 21, No. 3, 1984, pp. 287-292.
- ⁸ O. Kern and S.G. Bilen, "Model of Current Collection to Small Breaches in Electrodynamic-Tether Insulation," AIAA 2003-4947, 39th Joint Propulsion Conference, Huntsville, AL, 2003.
- ⁹ E. Choiniere, et al., "Measurement of Cross-Section Geometry Effects on Electron Collection to Long Probes in Mesosonic Flowing Plasmas," AIAA-2003-4950, 39th Joint Propulsion Conference, Huntsville, AL, 2003.
- ¹⁰ K.N. Leung, "Characterization of Ion Sources: Multi-cusp ("Bucket" Type) Ion Source," appears in Chap. 2, Section 6 of Handbook of Ion Sources, B. Wolf, Ed., CRC Press, New York, 1995. See also Chap. 2, Section 13, "Large Area Ion Sources," and references therein.
- ¹¹ Y. Okumura, et al., "High Magnetic-field, Large-Volume Magnetic Multipole ion-Source Producing Hydrogen-Ion Beams with High Proton Ratio," *Rev. Sci. Instrum.*, V. 55, No. 1, 1984, pp. 1-7. See also Y. Ohara, et al., "3D Computer Simulation of the Primary Electron Orbits in a Magnetic Multipole Plasma Source," *J. Appl. Physics*, V. 61, No. 4, 1987, pp. 1323-1328. Note that ring-cusp rather than line cusp magnetic field configurations are studied in these papers, which are similar to our plasma source and magnetic filter design. References that cite this family of ion sources also discuss the physics of electron temperature reduction across magnetic filters. e.g., M. Shirai, et al., "Theoretical Investigation of Electron Temperature Variation Across Magnetic Filter in a Negative Ion Source," *Rev. Sci. Instrum.*, V. 67, No. 3, 1996, pp. 1085-1087. And references therein.
- ¹² S.R. Walther, K.N. Leung, and W.B. Kunkel, "Production of Atomic Nitrogen Ion Beams," *Rev. Sci. Instrum.* V. 61, No. 1, 1990, pp. 315-317.
- ¹³ J.N. Matossian, "Plasma Ion-Implantation Technology at Hughes Research Laboratories, *J. of Vac. Sci. and Tech. B*, V. 12, No. 2, 1994, pp. 850-853.
- ¹⁴ Lee Y, et al., "Co-axial multicusp source for low axial energy spread ion beam production," *Nuclear Instruments and Methods in Physics Research, Section A- Accelerators, Spectrometers, Detectors, and Associated Equipment*, V. 433, No. 3, Sep. 1, 1999, pp. 579-586.
- ¹⁵ D.C. Ferguson, et al., "ISS FPP Ionospheric Electron Density and Temperature Measurements-Results, Comparison with the IRI-90 Model, and Implications of ISS Charging," AIAA-2003-1083, 41st Aerospace Sciences Meeting, Reno, Nevada, 2003. See also R. Mikatarian, et al.,

“Electrical Charging of the International Space Station,” AIAA-2003-1079, 41st Aerospace Sciences Meeting, Reno, Nevada, 2003

¹⁶ K.W. Ehlers and K.N. Leung, “Effect of a Magnetic Filter on Hydrogen-Ion Species in a Multicusp Ion-Source,” *Rev. Sci. Instrum.*, V. 52, No. 10, 1981, pp. 1452-1458.

¹⁷ E.P. Szuszczewicz and J.C. Holmes, “Surface Contamination of Active Electrodes in Plasmas: Distortion of Conventional Langmuir Probe Measurements,” *J. of Appl. Physics*, V. 46, 1975, pp. 5134-5143.

¹⁸ P. Gill and C.E. Webb, “Electron-Energy Distributions in Negative Glow and Their Relevance to Hollow-Cathode Lasers,” *J. of Appl. Physic D- Applied Physics*, V. 10, No. 3, 1977, pp. 299-311.

¹⁹ J.D. Swift and M.J.R. Schwar, Electrical Probes for Plasma Diagnostics, London Iliffe Books, American Elsevier Publishing Co., Inc., New York, 1969.